Desalination and Water Treatment
www.deswater.com
doi: 10.1080/19443994.2014.913998

55 (2015) 285–296
June

Taylor & Francis
Taylor & Francis Group

Parametric study and heat transfer mechanisms of single basin v-corrugated solar still

A.A. El-Sebaii[a], S.M. Shalaby[b,*]

[a]*Faculty of Science, Department of Physics, Tanta University, Tanta, Egypt, Tel. 00201069625914; email: ahmedelsebaii@yahoo.com (A.A. El-Sebaii)*
[b]*Faculty of Engineering, Department of Engineering Physics and Mathematics, Tanta University, Tanta, Egypt, Tel. +20 1223676159; email: saleh_shalaby@yahoo.com (S.M. Shalaby)*

Received 26 November 2013; Accepted 4 April 2014

ABSTRACT

A transient mathematical model was presented for a single basin solar still with v-corrugated basin liner. The model was based on an analytical solution of the energy balance equations for various elements of the still assuming the temperatures of the inner and outer surfaces of the still covers are not equal. The performance of the still was investigated by computer simulation using the climatic conditions of Tanta (lat. 30˚47′N, long. 31˚E), Egypt. The calculated results showed that the v-corrugated plate had improved both the daily productivity and daily efficiency by a relative percentage difference of approximately 24% compared to the case when a flat basin liner of the same area of 0.437 m^2 was used. Effects of basin water mass and the number, height, and the half angle of the "vee" on the daily productivity and efficiency of the still were studied. To validate the proposed mathematical model, the simulated results were compared with the results presented in the literature for a v-corrugated solar still. It was concluded that the proposed model is able to predict the still performance during sunshine hours with good accuracy.

Keywords: Single basin solar stills; V-corrugated; Computer simulation; Productivity

1. Introduction

Supplying fresh water is still one of the major problems in arid remote areas in different parts of the world. Solar stills can solve part of the problem in those areas where solar energy is available. Basin-type solar stills are simple in design and have low technology; hence, low maintenance expenses are required. Detailed reviews of different designs and factors affecting the performance of active and passive solar stills had been reported [1–3]. A review article describing the recent methods that had been used for improving solar still productivity was also recently presented by Velmurugan and Srithar [4]. All methods reported in these review articles aimed to improve the still productivity by reutilizing the latent heat of condensation [5], coupling the still to solar collectors [6] or solar ponds [7], using external and/or internal reflectors [8,9], reducing the volumetric heat capacity of the basin using different wick materials [10], using energy storage media [11–14], optimizing the insulation thickness [15], etc. A thermal analysis of a solar desalination system was carried out by Tiwari et al. [16] to optimize the glass cover inclination. They

*Corresponding author.

found that the optimum inclination of the glass cover during summer is 10˚ under Delhi climatic conditions and this angle is larger for winter months. The optimum inclination of the glass cover of the double slope solar still during winter is found to be 55˚ under Delhi climatic conditions as concluded by Singh et al. [17]. Various designs of solar stills were studied experimentally by Tiwari et al. [18]. They concluded that the multiwick solar still is the most economic and efficient one. Other method that can be used for enhancing the single effect solar still performance is the increase of basin liner area and/or the evaporation surface area of brine. Dev et al. [19] investigated experimentally and theoretically the thermal performance of an inverted absorber solar still for different basin water depths in an attempt to increase the area of the still absorber where both sides of the basin liner absorb the incident solar radiation. Other authors investigated the effect of increasing the surface area of evaporation of water on the performance of basin-type solar stills by using different wick materials [10] in the basin of a double slope solar still or using a vertical jute cloth at the middle of the basin of a regenerative solar still to utilize the latent heat of condensation released at the inner surface of the glass cover [11]. Moreover, Mahdi et al. [20] investigated experimentally a tilted wick-type solar still with charcoal cloth as an absorber/evaporator material and for saline water transport. It was concluded that increase of the input water mass flow rate leads to a reduction in the efficiency of the still where the representative daily efficiency of the still was 53% on a clear summer day. Omara et al. [21] performed an experimental study to compare the thermal performance of conventional single basin solar still with finned and v-corrugated solar stills. They found that the finned and v-corrugated solar stills give an increase in distilled water by 40 and 21%, respectively, compared with the conventional still. El-Zahaby et al. [22] investigated the thermal performance of a solar still on feeding the saline water into the still through a controlled transverse reciprocating spraying system in the form of droplets to spread on the top surface of a corrugated steeped shape absorber solar still. An accumulated productivity of 6.355 l/m^2 over 10 working hours with an efficiency of 77.35% was achieved.

Recently, Srivastava and Agrawal [23] investigated experimentally and theoretically the performance of the single sloped basin solar still using multiple floating porous absorbers. A sloped basin solar still with extended porous fins was also experimentally investigated by the same authors [24]. They indicated that the modified solar stills perform better than the conventional basin-type solar still.

It is indicated from the previous studies that, using v-corrugated plates as basin liners in solar stills considerably enhance their daily productivity and efficiency. However, detailed study about the effect of the configuration parameters of the v-corrugated absorber such as the v-height, number of “vees”, and the v-angle on the still productivity was not presented in the literature. Also, as far as the author knows, the dependence of the heat transfer rate from the v-corrugated basin liner to the brine on these parameters is not investigated previously. Therefore, the main objective of the present work is to develop a computer model for a v-corrugated single basin solar still in an attempt to increase the basin liner surface area; hence, the amount of heat transfer from the v-corrugated basin liner to the water increases. Effects of the v-configuration parameters and the mass of basin water m_w on the daily productivity of the still were studied. The theoretical model was validated by comparing the calculated results with that found in the literature [21].

2. Thermal analysis

A schematic diagram of the v-corrugated single basin solar still is shown in Fig. 1. The basin liner of the still consists of a v-corrugated black painted galvanized iron sheet of thickness 2 mm. The bottom and sides of the basin are insulated by 3 cm layer of sawdust contained in a wooden frame of 1 cm thickness. The cover of the still is made up of 3 mm thick soda glass, making an angle of 10˚ with horizontal (the still

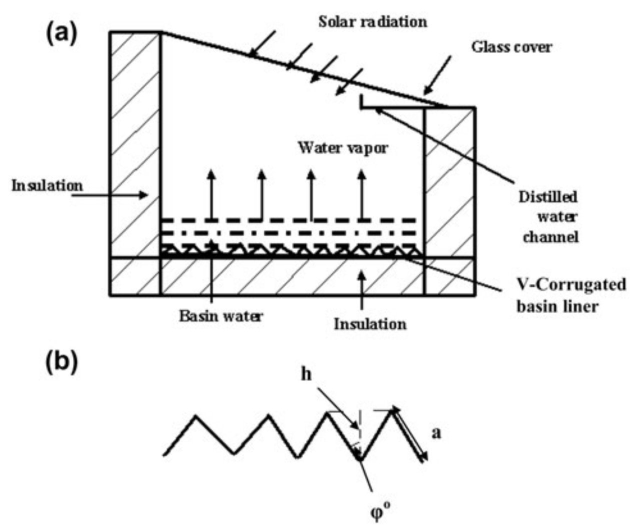

Fig. 1. (a) The single basin solar still with v-corrugated basin liner; (b) part of the v-corrugated basin liner (h is the v-height, a is the v-length, and φ is the half angle of the “vee”).

is investigated during summer days). The fresh water is collected in an aluminum channel fixed at the lower end of the glass cover. The still is oriented to face south to allow for the still cover to receive most of the available solar radiation. The solar radiation transmitted through the glass cover and basin water is absorbed by the v-corrugated basin liner; hence, its temperature increases. Part of thermal energy is transferred by convection to the basin water and the other will be transferred by conduction to the ground. The basin water transfers heat to the inner surface of the glass cover by radiation, convection, and evaporation. The heat is conducted through the cover and then transfers from the upper surface of the glass cover to surroundings by radiation to the sky and by convection to ambient air. The conventional solar still is similar to the v-corrugated one except the v-corrugated basin liner is replaced by a flat plate of a black painted galvanized iron sheet.

2.1. Mathematical models

When writing the energy balance equations for the various elements of the conventional and v-corrugated stills the following assumptions are made:

(1) the heat capacities of basin liner, glass cover, and insulating material are negligible compared to that for the basin water;
(2) the side losses are negligible and the still is vapor tight;
(3) there is no temperature gradient across the thickness of basin water.

2.1.1. The conventional still

On the basis of the above assumptions, the energy balance equations for the various elements of the still basin may be written as follows:

Inner surface of the glass cover [25]:

$$I\alpha_g A_g + (h_{ewgi} + h_{cwgi} + h_{rwgi})A_w(T_w - T_{gi}) = \left(\frac{k_g}{x_g}\right)A_g(T_{gi} - T_{go}) \tag{1}$$

Outer surface of the still cover:

$$\left(\frac{k_g}{x_g}\right)A_g(T_{gi} - T_{go}) = h_{rgos}A_g(T_{go} - T_s) + h_{cgoa}A_g(T_{go} - T_a) \tag{2}$$

Basin water:

$$I\tau_g\alpha_w A_w + h_{cpw}A_p(T_p - T_w) = (h_{ewgi} + h_{cwgi} + h_{rwgi})A_w(T_w - T_{gi}) + m_w C_w \frac{dT_w}{dt} \tag{3}$$

where I is the total solar radiation incident on the still cover. The radiative h_{rwgi}, convective h_{cwgi}, and evaporative h_{ewgi} heat transfer coefficients are calculated using the following correlations due to Dunkle [26]:

$$h_{rwgi} = 0.9\sigma(T_w^2 + T_{gi}^2)(T_w + T_{gi}) \tag{3a}$$

$$h_{cwgi} = 0.884\left[(T_w - T_{gi}) + \left(\frac{p_w - p_{gi}}{2016 - p_w}\right)T_w\right]^{\frac{1}{3}} \tag{3b}$$

$$h_{ewgi} = 9.15 \times 10^{-7}\left[\frac{h_{cwgi}(p_w - p_{gi})L_w}{(T_w - T_{gi})}\right] \tag{3c}$$

where p_w and p_{gi} are the partial pressures of saturated vapor at the basin water and inner surface of the glass cover temperatures, respectively; L_w is the latent heat of vaporization of water. The convective heat transfer coefficient from the basin liner to the basin water h_{cpw} is calculated using the following correlation [27] by treating the basin liner as a horizontal plate facing up:

$$h_{cpw} = (0.54k_w/b)(\mathrm{Gr\,Pr})^{0.25} \tag{3d}$$

where Gr and Pr are Grashoff and Prandtl dimensionless numbers, respectively. b is the characteristic length taken as the width of the basin liner.

Basin liner;

$$I\tau_g\tau_w\alpha_p A_p = h_{cpw}A_p(T_p - T_w) + U_b A_p(T_p - T_a) \tag{4}$$

where $U_b = k_b/x_b$ is the back loss coefficient. k_b and x_b are the thermal conductivity and thickness of the insulating material.

From Eqs. (1), (2) and (4), T_{gi}, T_{go} and T_p are obtained as:

$$T_{gi} = \frac{I\alpha_g A_g + h_2 A_w T_w + U_g A_g T_{go}}{h_2 A_w + U_g A_g} \tag{5}$$

$$T_{go} = \frac{U_g T_{gi} + h_{rgos}T_s + h_{cgoa}T_a}{U_g + h_3} \tag{6}$$

$$T_p = \frac{I\tau_g\tau_w\alpha_p + h_{cpw}T_w + U_b T_a}{h_{cpw} + U_b} \tag{7}$$

where $h_2 = h_{rwgi} + h_{cwgi} + h_{ewgi}$ is the total internal heat transfer coefficient from the basin water to the lower surface of the glass cover and $h_3 = h_{rgos} + h_{cgoa}$ is the total external heat transfer coefficient. $U_g = (k_g/x_g)$ is the conductive heat transfer coefficient between the inner and outer surfaces of the glass cover, and k_g and x_g are the thermal conductivity and thickness of the cover. Substituting T_{gi}, T_{go}, and T_p and using Eqs. (5)–(7), Eq. (3) is obtained as:

$$\overline{f(t)} - aT_w = m_w C_w \frac{dT_w}{dt} \tag{8}$$

where $\overline{f(t)}$ is the average values of $f(t)$ during a time interval Δt and may be treated as a constant [25,28]. Mathematical expressions for $f(t)$ and a which are functions of solar intensity, ambient temperature, various heat transfer coefficients, etc. are given as:

$$f(t) = \left\{ \left(I\tau_g \alpha_w A_w + \frac{I\tau_g \alpha_p \tau_w A_p h_{cpw}}{U_b + h_{cpw}} + \frac{I\alpha_g A_w A_g h_2}{h_2 A_w + U_g A_g} + \frac{U_b A_p h_{cpw}}{h_{cpw} + U_b} T_a + \frac{h_2 U_g A_w A_g T_{go}}{h_2 A_w + U_g A_g} \right) \right\} \tag{9}$$

$$a = \frac{U_b A_p h_{cpw}}{h_{cpw} + U_b} + \frac{h_2 A_w A_g U_g}{h_2 A_w + U_g A_g} \tag{10}$$

Eq. (8) is solved analytically under the following initial condition

$$T_w(t = 0) = T_{wi} \tag{11}$$

where T_{wi} is the initial temperature of basin water. The following formula has been obtained for the basin water temperatures T_w,

$$T_w = \frac{\overline{f(t)}}{a} \left\{ 1 - \exp\left(\frac{-at}{X} \right) \right\} + T_{wi} \exp\left(\frac{-at}{X} \right) \tag{12}$$

Mathematical expression for X which is function of solar intensity, ambient temperature, various heat transfer coefficients, etc. is given as:

$$X = m_w C_w \tag{13}$$

2.1.2. The v-corrugated still

The energy balance equations for the v-corrugated still are similar to those for the conventional still except the basin liner heat transfer area A_p for the v-corrugated basin liner may be calculated using the following equation:

$$A_p = 2Nhb/\cos\varphi \tag{14}$$

while the still area exposed to solar radiation is obtained as:

$$A_{\exp} = 2Nhb \tan\varphi \tag{15}$$

where N is the number of "vees", h is the v-height, φ is the half angle of the "vee", and b is the basin liner width which is taken equals 1 m for both the conventional and v-corrugated stills. The factor 2 in Eq. (14) and (15) because each "vee" has two sides with the same surface area . Furthermore, the correlation given by Eq. (3d) that was used for calculating the convective heat transfer coefficient from the flat basin liner to the basin water h_{cpw} for the conventional still is not valid for the v-corrugated plate. Therefore, h_{cpw} in case of the v-corrugated still is calculated by treating each "vee" as it is composed of two sides, each of them makes an angle φ with the vertical axis as shown in Fig. 1(b). Hence, for each side of the "vee", Nusselt number is calculated using the following correlation [27]

$$N_u = 0.8(\mathrm{GrPr})^{0.25} \left[\frac{\cos\varphi}{1 + \left(1 + \frac{1}{\sqrt{Pr}} \right)^2} \right]^{0.25} \tag{16}$$

where Gr and Pr are the Grashoff and Prandtel dimensionless numbers calculated using the following equations [27]:

$$\mathrm{Gr} = \frac{g\beta\rho^2 d^3 \Delta T}{\mu^2} \tag{17}$$

$$\mathrm{Pr} = \mu C_w / k_w \tag{18}$$

where d is the characteristic length and is taken to be equals the v-height (h), ΔT is the temperature difference between the heating surface and fluid. The meaning of other symbols is given in the nomenclature. The heat transfer coefficient h_{cpw} is then given by:

$$h_{cpw} = Nu \cdot k_w / d \tag{19}$$

The rate of heat transfer Q_{cpw} from the basin liner to the basin water is therefore calculated with the aid of the following formula:

$$Q_{cpw} = h_{cpw} A_p (T_p - T_w) \tag{20}$$

2.2. Productivity and efficiency of the still

The hourly productivity P_h for both the conventional and v-corrugated stills is calculated using the following Eq.

$$P_h = h_{ewgi}(T_w - T_{gi}) \times 3,600/L_w \tag{21}$$

The daily productivity P_d and the daily efficiency η_d are calculated using the following formulas

$$P_d = \sum_{24hrs} P_h \tag{22}$$

$$\eta_d = \frac{P_d L_{w,av}}{(A_{\exp} \sum I)\Delta t} \times 100 \quad (\%) \tag{23}$$

where $L_{w,av}$ is the daily average of the latent heat of vaporization of water and Δt is the time interval during which the solar radiation is measured.

3. Numerical calculations

Fig. 2 shows the hourly variations of solar radiation intensity incident on a horizontal surface I_h and ambient temperature T_a on a typical day of August 2009 (29/8/09) for Tanta (Egypt). The horizontal solar radiation I_h was measured using an Epply EPSP pyranometer coupled to an Epply instantaneous solar radiation meter Model No. 455 with sensitivity of 8.79×10^{-6} (V/W m^2) and accuracy better than 5% in the range from 0 to 2000 W/m^2. The ambient temperature T_a was measured using a mercury thermometer with accuracy 0.5˚C. The solar radiation data were employed for numerical calculations where a computer simulation, based on Liu and Jordan isotropic model [29], was prepared in Pascal language by writing subroutines for calculation of global solar radiation incident on the still cover I using the hourly measured values of I_h. Another computer program was developed also in Pascal language for the solution of energy balance equations of the still elements. The values of the relevant parameters [27,29] used for numerical calculations are summarized in Table 1.

Numerical calculations were started at 8:00 AM assuming the initial temperatures of various components of the still to be equal to ambient temperature. Using known initial values for the various temperatures, different internal and external heat transfer coefficients were calculated. Using these values of heat transfer coefficients along with climatic parameters, the basin linear, basin water, and inner and outer surfaces of the glass cover temperatures were calculated for a time interval Δt (10 min). Numerical calculations indicated that decreasing the time interval beyond 10 min does not significantly improve the accuracy of estimation of the still performance. The hourly productivity P_h and rate of heat transfer from the basin liner Q_{cpw} were then calculated by using Eqs. (21) and (20), respectively. The procedure was repeated for an additional time interval Δt and so on, until 8:00 AM of the next day. The daily productivity and daily efficiency were then calculated by using Eqs. (22) and (23). Numerical calculations had been performed for different v-configuration parameters in order to study the effect of these parameters on productivity for various masses of basin water in the range 5–200 kg. Thermal performances for the conventional and v-corrugated stills were compared under the same climatic conditions. In an attempt to validate the proposed mathematical models, the obtained theoretical results for both the conventional and v-corrugated stills were compared with the experimental results that were presented in the literature [21] under the same climatic and operating parameters.

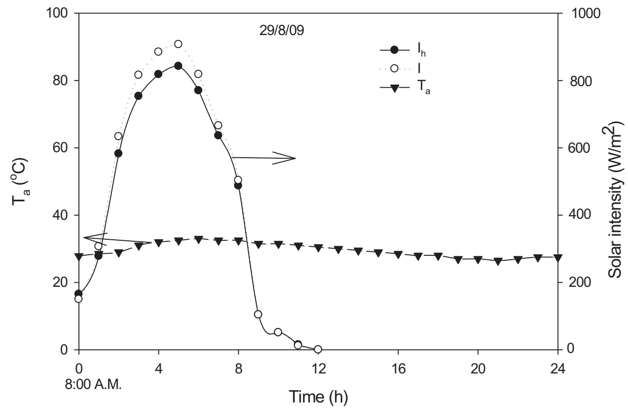

Fig. 2. Hourly variations of measured total solar radiation incident on a horizontal surface (I_h) and still cover (I), and ambient temperature (T_a) on a typical day of August (29/8/09) in Tanta (Egypt).

4. Results and discussion

Numerical calculations have been performed for the stills on a typical day of August in Tanta (Egypt). The measured ambient temperature T_a and solar

Table 1
Relevant parameters used for numerical calculations [27,29]

Relevant parameter	Value	Relevant parameter	Value
A_p (conventional still)	1 m^2	α_g	0.05
τ_g	0.90	k_s (W/m K)	0.059
τ_w	0.95	x_s (m)	0.05
α_p	0.90	C_w (J/kg K)	4,190
α_w	0.05	k_g (W/m K)	1.05
σ (W/m^2 K^4)	5.669×10^{-8}	L_g (m)	0.003
V (m/s)	3.0	k_w (W/m K)	0.628

radiation data that were employed for numerical calculations are presented in Fig. 2. From the results of Fig. 2, it is seen that the solar radiation incident on the still cover I achieves maximum and daily average values of 906.9 and 450.1 W/m^2, respectively. The maximum and daily average values of T_a are 33 and 29.6℃, respectively. Fig. 3(a) summarizes comparisons between the temperatures of the various elements of the conventional and v-corrugated stills for the same area exposed to solar radiation when the number of "vees" N, v-height h, and the v-half angle φ equal 20, 3 cm, and 20˚, respectively. The v-corrugated still area exposed to solar radiation is obtained as 0.437 m^2 as calculated from Eq. (15). The temperatures of the stills elements increase as the solar radiation increases until they achieve their maximum values around the noon time and then decrease with the decrease of solar radiation I and ambient temperature T_a. It is also seen that, the temperatures of the elements of the v-corrugated still are higher than those for the conventional still due to the increased amount of solar radiation absorbed by the corrugated absorber which causes an increase in the water glass temperature differences ΔT_{wgi} as shown in Fig. 3(b). The increase in ΔT_{wgi} is pronounced during sunshine hours as expected where the maximum and daily average values of ΔT_{wgi} are found to be 25.8 and 8.2℃, respectively, for the modified still compared to 22.4 and 7.3℃ in case of the conventional still (see Fig. 3(b)). The increase in ΔT_{wgi} causes an increase in the hourly productivity P_h of the modified still particularly during sunshine hours as shown in Fig. 3(c). The maximum values of P_h are obtained as 0.896 and 0.662 (kg/m^2 h) for the modified and conventional stills, respectively. After sunset, the productivities of the modified and conventional stills are almost equal. When the mass of basin water m_w equals 50 kg, the daily productivities P_d of the modified and conventional stills, calculated from the results of Fig. 3(c), are found to be 5.296 and 4.027 (kg/m^2 d) with daily efficiencies η_d of 62.2 and 47.3%, respectively. Therefore, the v-corrugated plate has improved both of the P_d and η_d by a relative percentage difference of approximately 24% compared to the case when a flat basin liner is used. Omara et al. [21] concluded that, the accumulated productivity of the v-corrugated solar still is higher than that of the traditional still by about 21%.

Hourly variations of the evaporative heat transfer coefficients from basin water to the inner surface of the glass cover h_{ewgi} and the total internal heat transfer coefficient h_2 for the modified and conventional stills when $m_w = 50$ kg, $N = 20$, $h = 3$ cm, and $\varphi = 20^\circ$ are presented in Fig. 4(a). It is clear from the results of Fig. 4(a) that h_{ewgi} and hence h_2 for the modified still are higher than those for the conventional still especially during the period from 8:00 AM until midnight; probably, due to the increased water–glass temperature difference in case of the modified still. The maximum values for h_{ewgi} and h_2 are obtained as 24.32 and 33.88 (W/m^2 K) for the modified still compared to 20.60 and 29.85 (W/m^2 K) for the conventional still. It is worth mentioning that, the other internal and external heat transfer coefficients (h_{cwgi}, h_{rwgi}, and h_{cgoa}) are almost equal for both stills because these heat transfer coefficients are less dependent on temperature [30]. Although the values of the convective heat transfer coefficient from the basin liner to the basin water h_{cpw} for the modified still are found to be lower than those for the conventional still during sunshine hours (see Fig. 4(b)), Q_{cpw} behaves in a reverse manner where it is found to be higher than those for the conventional still during sunshine hours and overnight period as shown in Fig. 4(b). The maximum and daily average values for h_{cpw} equal 235.85 and 140.25 (W/m^2 K) for the modified still compared to 307.15 and 180.98 (W/m^2 K) for the convention still. The corresponding values of Q_{cpw} are obtained as 867.33 and 230.02 W for the modified still compared to 684.95 and 183.03 W for the conventional still. The temperature potential ($T_p - T_w$) for convective heat transfer in case of the modified still is greater than that for the conventional still (see Fig. 3(a)).

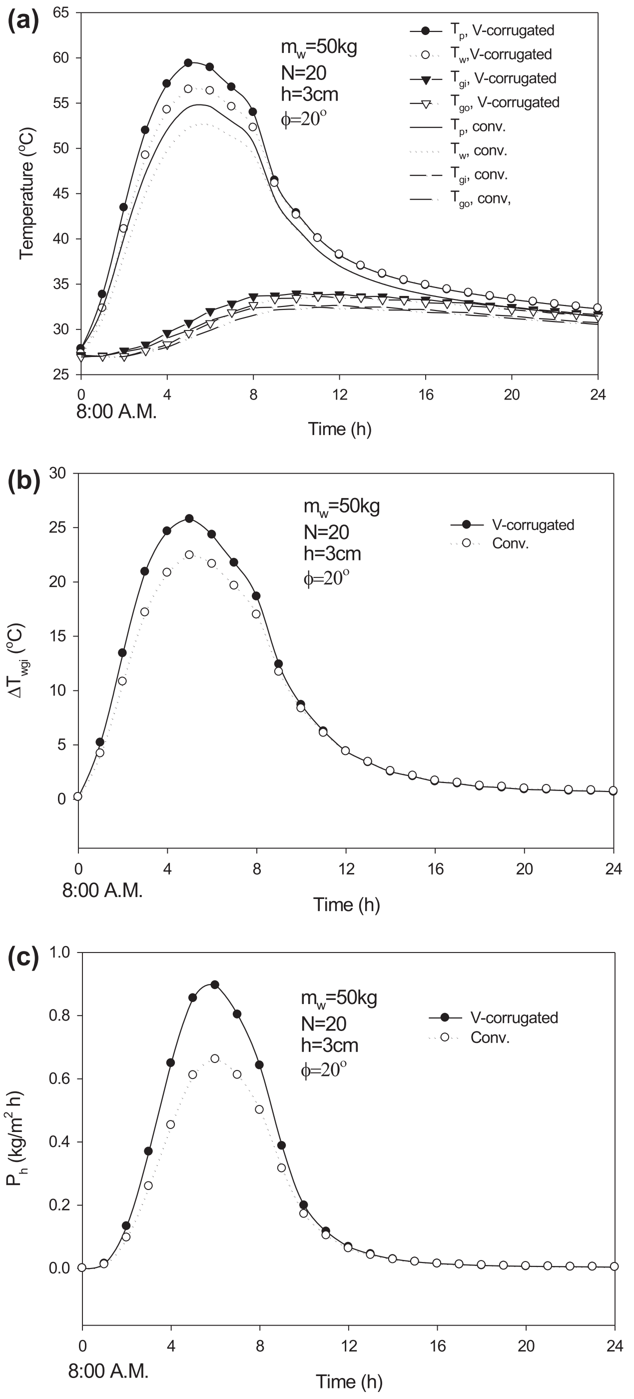

Fig. 3. (a) Variations of calculated temperatures of the conventional and v-corrugated stills; (b) variations of water–glass temperature difference of the conventional and v-corrugated stills; (c) variations of the hourly productivity of the conventional and v-corrugated stills on a typical day of August 2009.

To validate the proposed mathematical models, the thermal performance of the v-corrugated and conventional stills has been compared with the experimental

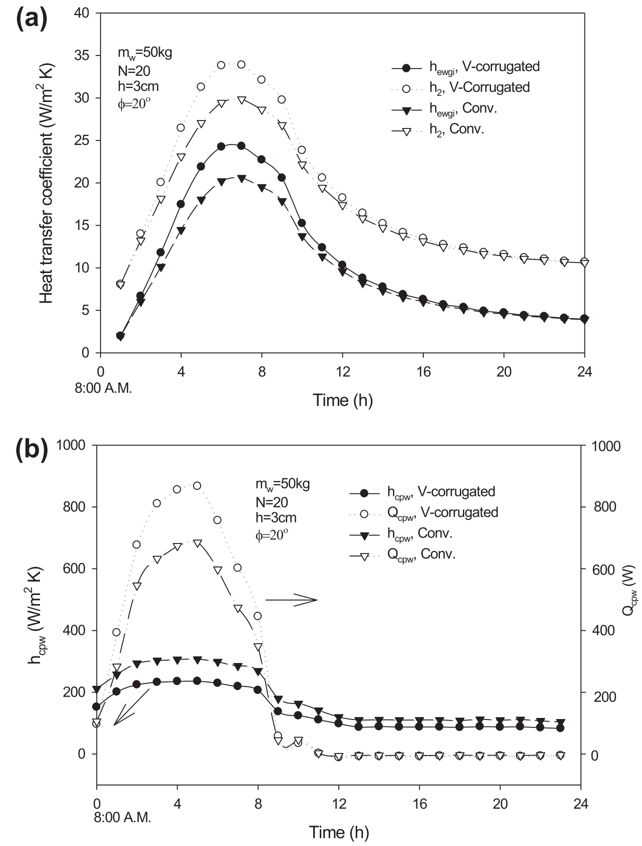

Fig. 4. Hourly variations of heat transfer coefficients and rate of heat transfer from the basin line of the v-corrugated and conventional solar stills on a typical day of August 2009.

results that were obtained for conventional and modified unit with a v-corrugated absorber with an area of 0.8 m^2, $N = 19$, $h = 5$ cm, and $\varphi = 40^\circ$ under the prevailing weather conditions of Kafr Elsheekh city (40 km away from Tanta and has a latitude of 30˚6´N), Egypt [21]. Examples for such comparisons are shown in Fig. 5 on a typical day of July (8/7/2010). The authors of Ref. [21] were conducted their measurements only during sunshine hours. It is clear from the results of Fig. 5 that the agreement between the present results and those found in the literature [21] is fairly good. Even though, there are some differences due to uncertainties in correlations used for calculations of various heat transfer coefficients and solar radiation incident on the stills covers. Temperature gradient within the basin water and heat capacities of the basin liner, glass cover, and insulation materials are not considered in the mathematical analysis and they represent another source of error. The comparisons shown in Fig. 5 clearly confirm that the proposed mathematical model for the v-corrugated still and the method proposed for

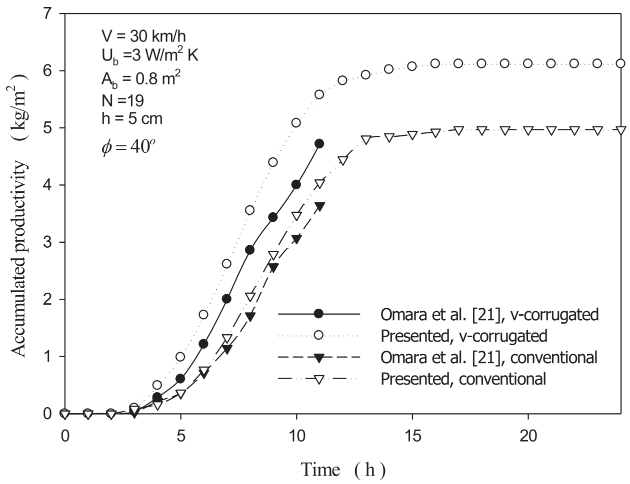

Fig. 5. Comparisons between the calculated (presented) and measured (Omara et al. [21]) accumulated productivity of basin water of the conventional and v-corrugated solar still on 8/7/2010.

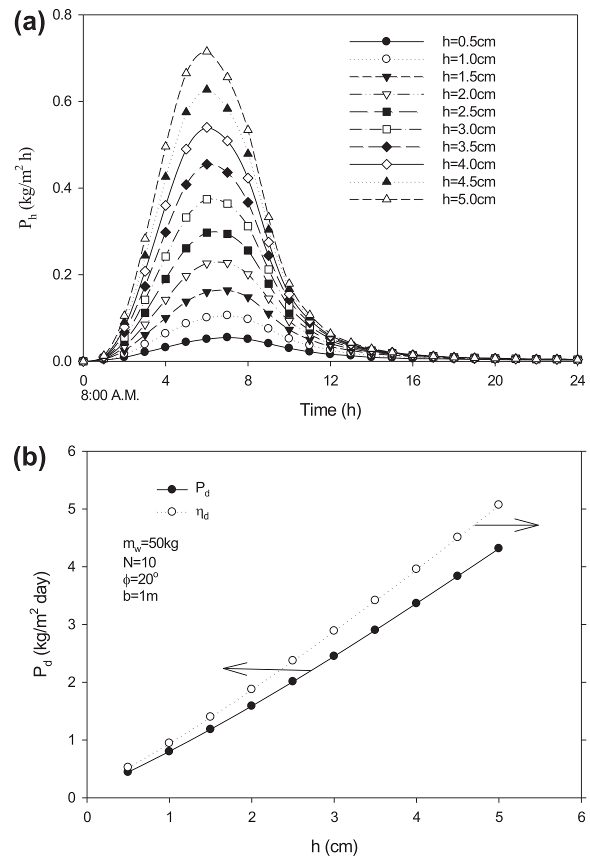

Fig. 6. (a) Dependence of hourly productivity on the v-height (h); (b) dependence of the daily productivity and efficiency of the v-corrugated still on the v-height (h).

calculation of the convective heat transfer coefficient from the v-corrugated basin liner h_{cpw} may be used for investigating the thermal performance of v-corrugated solar stills with a reasonable accuracy.

The main objective of the present paper is to investigate the effect of the "vee" configuration parameters on the still performance. Fig. 6(a) shows variations of the hourly productivity P_h with time for different v-heights h when $m_w = 50$ kg, $N = 10$, and $\varphi = 20^{\circ}$. The dependence of the daily productivity P_d and efficiency η_d on h is summarized in Fig. 6(b). P_h increases as h increases due to the increased A_{exp} with increasing h (see Eq. (15)) and hence, the amount of solar radiation absorbed by the basin liner increases. The heat transfer area A_p is also increases with increasing h (see Eq. (14)) causes an increase in the rate of heat transfer from the basin liner to the basin water Q_{cpw}; consequently, both P_d and η_d are found to increase almost linearly with increasing h as shown in Fig. 6(b). The maximum value of P_h increases from 0.055 to 0.715 (kg/m^2 h) with increasing h from 0.5 to 5 cm. The corresponding increase in A_p is from 0.1064 to 1.0641 m^2. On the other hand, P_d and η_d are increased from 0.444 and 5.26 to 4.315 (kg/m^2 day) and 50.70% on increasing h from 0.5 to 5 cm, respectively. The following quadratic correlation between P_d and h has been obtained:

$$P_d = 0.073 + 0.702h + 0.0296h^2;\ r^2 = 0.99996 \quad \text{for}(0 < h \leq h \leq \text{cm}) \tag{24}$$

Variations of the hourly productivity P_h, evaporative rate of heat transfer Q_{ewgi}, and the daily productivity P_d and efficiency η_d for different numbers of the "vees" N are presented in Fig. 7 when $m_w = 50$ kg, $h = 3$ cm, and $\varphi = 20^{\circ}$. It is obvious from the results of Fig. 7(a) that, P_h increases with increasing N during sunshine hours; again, due to the increased area of the basin liner and the amount of the absorbed solar radiation which result in an increase in the water–glass temperature difference and hence, the rate of the evaporative heat transfer Q_{ewgi} increases with increasing N as seen in Fig. 7(b). After sunset, both P_h and Q_{ewgi} become independent on N as expected. In a similar manner to the dependence of P_d and η_d on h, the P_d and η_d are seen to increase continuously with increasing N (see Fig. 7(c)). P_d is found to increase from 1.183 to 8.679 (kg/m^2 day) with a corresponding increase in η_d from 13.99 to 100% with increasing N from 5 to 31. The value of $N = 31$ gives double heat transfer area for the modified still basin liner compared to that of the conventional still of the same

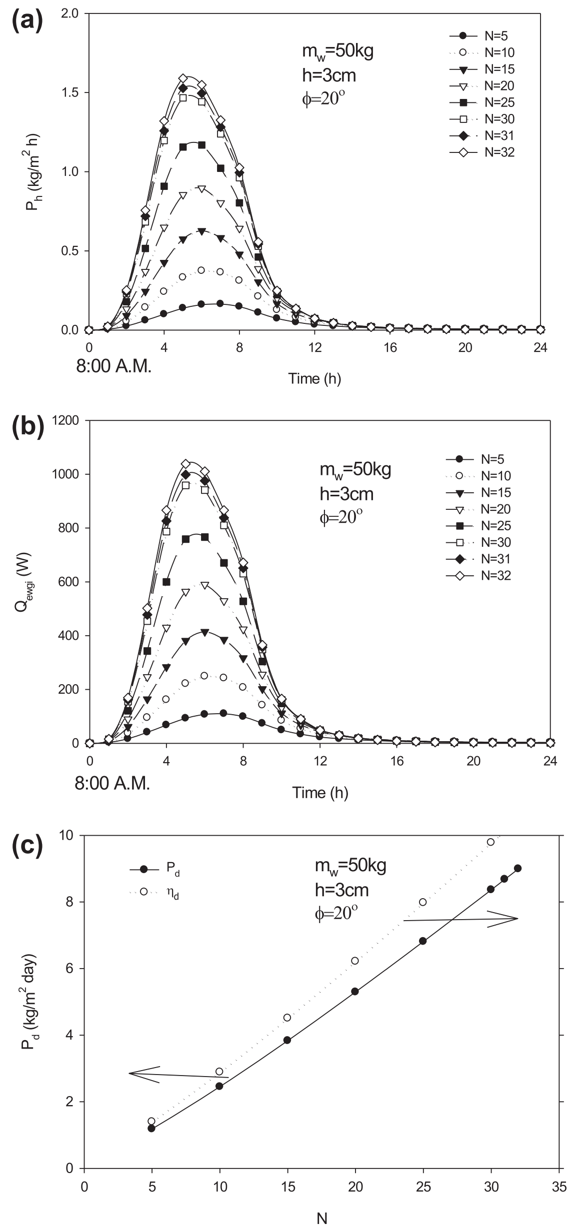

Fig. 7. (a) Dependence of hourly productivity on the number of “vees” (N); (b) dependence of evaporative heat transfer on the number of “vees”; (c) dependence of daily productivity and efficiency of the v-corrugated still on the number of “vees”.

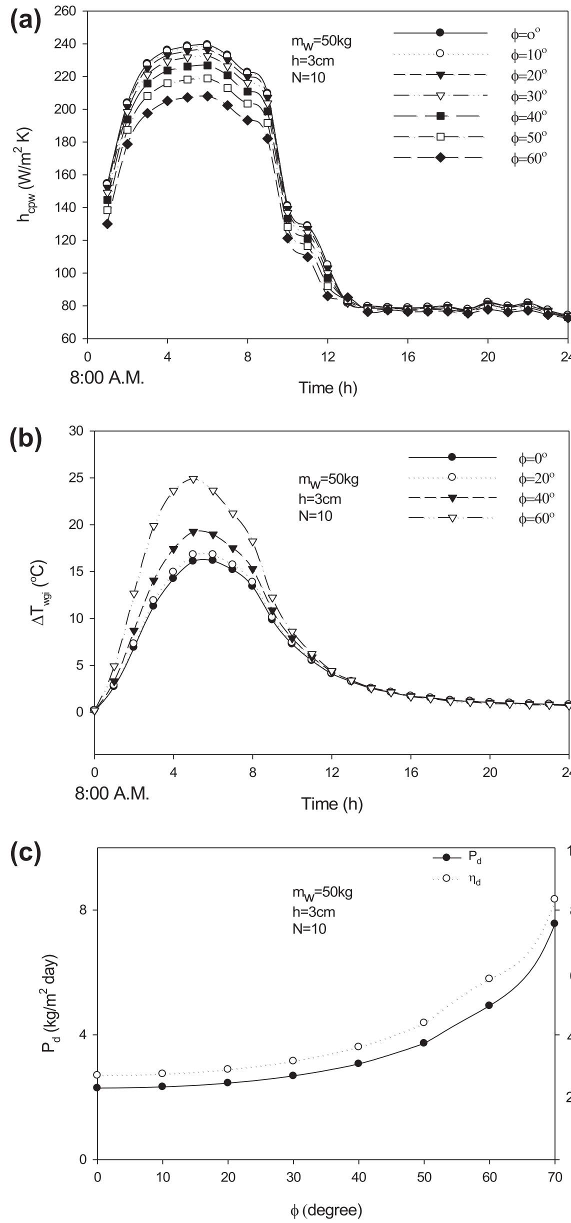

Fig. 8. (a) Dependence of h_{cpw} on the angle φ; (b) dependence of water–glass temperature difference on the angle φ; (c) dependence of the daily productivity P_d and efficiency η_d on the angle φ on 29/8/09.

exposed area. The following correlation between P_d and N has been obtained using the least square curve fitting technique:

$$P_d = -0.0773 + 0.242N + 1.3069N^2;\ r^2 = 0.99997 \quad \text{for}(1 \le N \le 32) \tag{25}$$

Hourly variations of the convective heat transfer coefficient from the basin liner to the basin water h_{cpw} for different values of the angle φ are summarized in Fig. 8(a) when $N = 10$, $h = 3$ cm, and $m_w = 50$ kg. It is seen that during sunshine hours, h_{cpw} slightly decreases with increasing φ until 40° beyond which h_{cpw} starts to decrease faster with increasing φ. Overnight, h_{cpw} is almost less dependent on φ. These results may be interpreted in terms of Eqs. (16)–(19) where h_{cpw} is directly proportional to $\cos\varphi$ to the power 0.25 and $\cos\varphi$ decreases slightly for low values of φ and then show very fast decrease for higher values of φ to approaches zero when $\varphi = 90^\circ$. Although h_{cpw} decreases with increasing φ, the rate of the convective heat transfer from the basin liner to the basin water Q_{cpw} is found to increase with increasing φ. On the other hand, the water–glass temperature difference ΔT_{wgi} is also found to increase during sunshine hours with increasing φ as shown in Fig. 8(b). The maximum values of ΔT_{wgi} are obtained as 16.2, 16.8, 19.2, and 24.9°C when φ equals 0, 20, 40, and 60°, respectively. Furthermore, the basin liner area A_p is inversely proportional to $\cos\varphi$ (see Eq. (14)), thus, A_p increases and also the amount of the absorbed solar radiation increases with increasing φ. Therefore, the daily productivity P_d and efficiency η_d show the behavior of an exponential growth function with increasing φ as shown in Fig. 8(c) due to the slight decrease in $\cos\varphi$ at lower values of $\varphi \leq 40^\circ$ and the fast decrease afterwards ($40^\circ < \varphi < 90$). The following single exponential growth correlation between P_d and φ has been obtained:

$$P_d = 2.498 + 9.51 \times 10^{-3} \exp^{9.073\times10^{-2}} \varphi;\ r^2 = 0.9971 \quad \text{for}(0 < \varphi \leq 70) \tag{26}$$

The dependence of P_d and η_d for the conventional and v-corrugated stills on the mass of basin water m_w when $N = 20$, $h = 3\,\text{cm}$ and $\varphi = 30^\circ$ on 29/8/09 is depicted in Fig. 9. It is clear from the results of Fig. 9 that P_d and η_d for both stills decrease almost linearly with increasing m_w due to the increased heat capacity of basin water with increasing m_w. For all values of m_w, the values of P_d and η_d for modified still are considerably higher than those for the conventional still. Therefore, by proper choice for the "vee" parameters, the productivity and efficiency of deep basins solar stills can be improved by replacing the flat basin liner by the v-corrugated one.

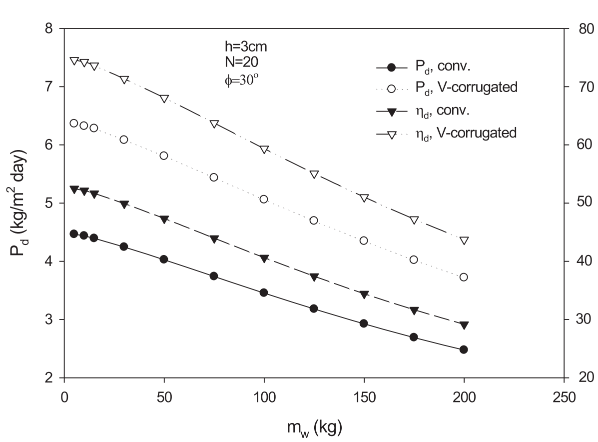

Fig. 9. Variations of daily productivity P_d and efficiency η_d on the mass of basin water m_w on 29/8/09.

5. Conclusions

Mathematical models for single basin conventional and v-corrugated stills are presented. The models are validated by making comparisons with the results found in the literature and performed for the stills under similar climatic conditions. The effects of the "vee" configuration parameters on the still performance are studied. It is concluded that:

(i) The v-corrugated plate has improved both of the P_d and η_d by a relative percentage difference of approximately 24% compared to the case when a flat basin liner is used when $A_{\text{exp}} = 0.437\,\text{m}^2$.

(ii) The daily productivity P_d increases almost linearly with increasing the number of "vees" N and v-height h; but, it shows some exponential growth with increasing the v-half angle φ.

(iii) For all investigated masses of basin water, P_d for the v-corrugated still is higher than that for the conventional still.

(iv) The v-corrugated basin liner should be used during sunshine hours to improve the productivity of deep basin solar stills with a v-height less than the depth of basin water to avoid the decrease in the evaporation surface area of basin water.

(v) By proper choice of the "vee" configuration parameters, the productivity of basin-type solar still has been improved significantly.

(vi) The proposed model for the v-corrugated still could be used for investigating the v-corrugated solar stills performances with good accuracy. It is advisable to use shallow depths of basin water to reduce the thermal inertia of basin water and improve the still efficiency.

Nomenclature

A	—	area (m^2)
A_{exp}	—	still area exposed to solar radiation
b	—	width of the basin liner (m)
C	—	specific heat (J/kg K)
d	—	characteristic length (m)
g	—	acceleration due to gravity (m/s^2)
Gr	—	Grashoff number
h	—	heat transfer coefficient (W/m^2 K), v-height (m)
I	—	solar radiation intensity (W/m^2)
k	—	thermal conductivity (W/m K)
L	—	latent heat (J/kg)
m	—	mass (kg)
N	—	number of “vees”
Nu	—	Nusselt number
P	—	productivity (kg/m^2)
p	—	vapor pressure (N/m^2)
Pr	—	Prandtl number
Q	—	rate of heat transfer (W)
T	—	temperature (℃)
t	—	time (s)
U	—	heat loss coefficient (W/m^2 K)
V	—	wind speed (m/s)
x	—	thickness (m)

Subscripts

a	—	ambient
av	—	average
b	—	back
c	—	convection
d	—	daily
e	—	evaporation
g	—	glass
h	—	hourly, horizontal
i	—	inner, initial
o	—	outer
p	—	basin liner
r	—	radiation
s	—	insulation, sky
w	—	water

Greek

α	—	absorptivity
β	—	coefficient of thermal expansion (℃$^{-1}$)
ρ	—	density (kg/m^3)
φ	—	“vee” half angle (°)
τ	—	transmissivity
σ	—	Stefan–Boltzmann’s constant ($W/m^2 K^4$)
μ	—	fluid viscosity (kg/m s)
η	—	efficiency (%)

References

[1] K. Sampathkumar, T.V. Arjunan, P. Pitchandi, P. Senthilkumar, Active solar distillation – A detailed review, Renew. Sustain. Energy Rev. 14 (2010) 1503–1526.

[2] A. Kaushal, Varun, Solar stills: A review, Renew. Sustain. Energy Rev. 14 (2010) 446–453.

[3] T.V. Arjunan, H.S. Aybar, N. Nedunchezhian, Status of solar desalination in India, Renew. Sustain. Energy Rev. 13 (2009) 2408–2418.

[4] V. Velmurugan, K. Srithar, Performance analysis of solar stills based on various factors affecting the productivity – A review, Renew. Sustain. Energy Rev. 15 (2011) 1294–1304.

[5] A.A. El-Sebaii, Thermal performance of a triple-basin solar still, Desalination 174 (2005) 23–37.

[6] Z.S. Abdel-Rehim, A. Lasheen, Experimental and theoretical study of a solar desalination system located in Cairo, Egypt, Desalination 217 (2007) 52–64.

[7] A.A. El-Sebaii, M.R.I. Ramadan, S. Aboul-Enein, N. Salem, Thermal performance of a single-basin solar still integrated with a shallow solar pond, Energy Convers. Manage. 49 (2008) 2839–2848.

[8] T. Hiroshi, N. Yasuhito, Effect of inclination of external flat plate reflector of basin type still in winter, Sol. Energy 81 (2007) 1035–1042.

[9] A.A. El-Sebaii, M. Al-Dossari, A mathematical model of single basin solar still with an external reflector, Desalin Water Treat. 26 (2010) 250–259.

[10] K. Kalidasa Murugavel, K. Srithar, Performance study on basin type double slope solar still with different wick materials and minimum mass of water, Renewable Energy 36 (2011) 612–620.

[11] M. Sakthivel, S. Shanmugasundaram, T. Alwarsamy, An experimental study on a regenerative solar still with energy storage medium – Jute cloth, Desalination 264 (2010) 24–31.

[12] A.A. El-Sebaii, A.A. Al-Ghamdi, F.S. Al-Hazmi, A.S. Faidah, Thermal performance of a single basin solar still with PCM as a storage medium, Appl. Energy 86 (2009) 1187–1195.

[13] O. Ansari, M. Asbik, A. Bah, A. Arbaoui, A. Khmou, Desalination of the brackish water using a passive solar still with a heat energy storage system, Desalination 324 (2013) 10–20.

[14] M. Dashtban, F.F. Tabrizi, Thermal analysis of a weir-type cascade solar still integrated with PCM storage, Desalination 279 (2011) 415–422.

[15] A.J.N. Khalifa, A.M. Hamood, Effect of insulation thickness on the productivity of basin type solar stills: An experimental verification under local climate, Energy Convers. Manage. 50 (2009) 2457–2461.

[16] G.N. Tiwari, J.M. Thomas, E. Khan, Optimisation of glass cover inclination for maximum yield in a solar still, Heat Recovery Syst. CHP 14 (1994) 447–455.

[17] A.K. Singh, G.N. Tiwari, P.B. Sharma, E. Khan, Optimization of orientation for higher yield of solar still for a given location, Energy Convers. Manage. 36 (1995) 175–181.

[18] G.N. Tiwari, H.P. Garg, Studies on various designs of solar distillation systems, Sol .Wind Technol. 1 (1985) 161–165.

[19] R. Dev, S. Abdul-Wahab, G.N. Tiwari, Performance study of the inverted absorber solar still with water depth and total dissolved solid, Appl. Energy 88 (2011) 252–264.

[20] J.T. Mahdi, B.E. Smith, A.O. Sharif, An experimental wick-type solar still system: design and construction, Desalination 267 (2011) 233–238.

[21] Z.M. Omara, M.H. Hamed, A.E. Kabeel, Performance of finned and corrugated absorbers solar stills under Egyptian conditions, Desalination 277 (2011) 281–287.

[22] A.M. El-Zahaby, A.E. Kabeel, A.I. Bakry, S.A. El-Agouz, O.M. Hawam, Enhancement of solar still performance using a reciprocating spray feeding system – An experimental approach, Desalination 267 (2011) 209–216.

[23] P.K. Srivastava, S.K. Agrawal, Experimental and theoretical analysis of single sloped basin type solar still consisting of multiple low thermal inertia floating porous absorbers, Desalination 311 (2013) 198–205.

[24] P.K. Srivastava, S.K. Agrawal, Winter and summer performance of single sloped basin type solar still integrated with extended porous fins, Desalination 319 (2013) 73–78.

[25] G.N. Tiwari, V. Dimri, A. Chel, Parametric study of an active and passive solar distillation system: Energy and Exergy analysis, Desalination 242 (2009) 1–18.

[26] R.V. Dunkle, International Development in heat transfer, ASME Proceedings, Inter. Heat Transfer, Part V, University of Colorado, 1961, p. 895.

[27] H.Y. Wong, Handbook of Essential Formula and Data on Heat Transfer for Engineers, Longman, London, 1977.

[28] V.B. Sharma, S.C. Mullick, Estimation of heat-transfer coefficients, the upward heat flow, and evaporation in a solar still, J. Sol.Energy Eng. 113 (1991) 36–41.

[29] J.A. Duffie, W.A. Beckman, Solar Engineering of Thermal Processes, Wiley, New York, NY, 1991.

[30] G.N. Tiwari, S. Sinha, Parametric studies of active regenerative solar still, Energy Convers. Manage. 34 (1993) 209–218.